Investigation on Dynamic Point Selection Scheme Based on Proportional Fair Criteria

Takeshi Takemoto
Faculty of Engineering, Kagawa University

Nobuhiko Miki
Faculty of Engineering, Kagawa University

***Abstract*—The coordinated multipoint (CoMP) transmission is one of the promising techniques to increase the throughput of users located at the cell-edge. Among the CoMP transmission schemes, the dynamic point selection (DPS) combined with the dynamic point blanking (DPB) is investigated, since it can achieve superior performance with relatively small overhead. This paper proposes the DPS/DPB scheme based on the proportional fair (PF) criteria, which is effective to exploit the tradeoff between fairness and network performance. We derive the optimum DPS/DPB allocation scheme by solving the *convex* optimization problem based on the achievable *average* data rate of each user. The paper evaluates the performance of the proposed scheme in the simple environment using the one-dimensional model with two BSs $(M = 2)$, and shows that the proposed scheme works well. Furthermore, the extension of the proposed scheme to select the DPS/DPB user candidates, and to the inter-cell interference coordination is presented.**

I. Introduction

The data traffic over the mobile network is still increasing especially in the downlink e.g. [1], [2]. More advanced wireless technologies are required to accommodate such traffic. One of the most promising technologies is the coordinated multipoint (CoMP) transmission in the downlink, which can improve the throughput of users suffering the severe interference from other cells, i.e., the cell-edge user throughput [3], [4]. In the CoMP transmission, the multiple geophysically separated base stations (BSs) coordinate their transmission to the user. In the paper, we define such user as the CoMP user.

CoMP technologies can be classified into three schemes, i.e., coordinated scheduling and coordinated beamforming (CS/CB), joint transmission (JT), and dynamic point selection (DPS) [3]. In CS/CB, only one BS transmits data to the CoMP users, which is same as the ordinary non-CoMP transmission. The difference from the ordinary transmission is that the scheduling decisions of neighbouring BSs coordinate in order to reduce the interference by beamforming. Meanwhile, in JT CoMP, multiple BSs transmit data simultaneously to a CoMP user. In DPS CoMP, the transmission BS varies according to the changes in channel and interference conditions. These CoMP techniques can be combined with dynamic point blanking (DPB), which means that multiple BSs mutes/blanks the frequency/time resources to reduce the interference to the CoMP user. In all three CoMP schemes, the channel state information (CSI) for multiple BSs are required, which is generally fed back to the BS via the uplink channel. The amount of the CSI feedback required for CoMP transmission depends on the CoMP schemes. Among the CoMP techniques listed above, the DPS combined with DPB (DPS/DPB) is investigated in the paper. This is because the DPS/DPB can achieve superior performance with relatively small CSI overhead [4].

In the DPS/DPB scheme, the selection of the DPS users and DPB resources plays an important role to improve the throughput. In the paper, the proportional fair (PF) criteria [5] is used, which was originally proposed in the context of wired networks, and has been widely used to address the fairness issues in the wireless networks. This is because the PF criteria is effective to exploit the tradeoff between fairness and network performance. The PF criteria is represented by a local maximum of the logarithmic utility function [5]. When the single cell transmission, i.e., non-CoMP transmission, is applied, the scheduling between BSs is not coordinated. Therefore, even if the PF scheduling for each BS is performed independently, the logarithmic utility function can be maximized. However, when multi-cell transmission, i.e., the CoMP transmission is employed, the scheduling between BSs needs to be coordinated to maximize the utility function, which requires complex scheduling [6].

Regarding to the scheduling for the single-cell transmission, the optimum resource allocation is derived by solving the *convex* optimization problem, e.g., in [7], [8]. Furthermore, in [9], the optimum resource allocation for the multi-cell transmission employing JT is derived by solving the *convex* optimization problem, which becomes complex compared to the single-cell transmission, since the amount of resources of the cell is affected by the neighbouring cells in the the multi-cell transmission. Although the multi-cell transmission is considered in [9], the DPB is not taken into account, which improves the achievable data rate of all neighbouring cells at the sacrifice of the reduction of useful resources in the cell.

The paper tackles the complex *convex* optimization problem employing the DPB in addition to the multi-cell transmission, i.e., DPS. In other words, we solves the *convex* optimization problem employing the DPS/DPB transmission based on the achievable *average* data rate of each user with and without DPS/DPB. Although the proposed scheme is not directly applicable to the actual system, since it is not *instantaneous* data rate, but *average* data rate, it can be possible to apply to select the DPS/DPB user candidates based on the achievable *average* data rate of each user, and the inter-cell interference coordination (ICIC) [10], which will be discussed in Section IV.

The rest of paper is organized as follows. Section II describes the DPS/DPB scheme and system model, followed by the problem description and optimum allocation in Section III. One numerical evaluation applying this solution is presented in Section IV. Finally, Section V concludes the paper.

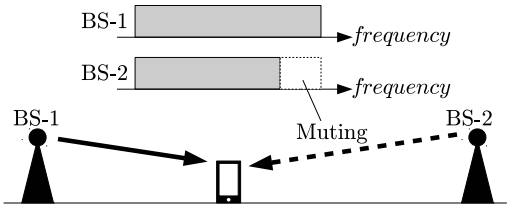

Fig. 1: DPS/DPB scheme.

II. DPS/DPB Scheme and System Model

In the paper, the following DPS/DPB scheme is assumed.

- Two BSs are coordinated at the same time, i.e., one BS transmits data to the user, and the other BS mutes corresponding resources.
- Power boosting is not employed for DPS resources, even if the transmission power is less than maximum transmission power.

Fig.1 shows one example when the BS-1 transmits data to the CoMP user, and the BS-2 mutes the corresponding resources to reduce the interference to the CoMP user.

Fig. 2 illustrates the system model with M BSs with DPS/DPB mentioned above. The total system bandwidth is divided into the non-muting bandwidth, $\mathcal{B}$, and the muting bandwidth, $\hat{\mathcal{B}}$, respectively. The muting bandwidth, $\hat{\mathcal{B}}$ is further divided into the muting bandwidth for the m-th BS, $\hat{\mathcal{B}}_m$. As shown in the figure, the resource in $\hat{\mathcal{B}}_m$ is not utilized at the m-th BS to improve the achievable data rate at other BSs. In other words, the resources in $\hat{\mathcal{B}}_l$ $(l \neq m)$ in addition to $\mathcal{B}$ is utilized for data transmission in the m-th BS. Furthermore, N users are assumed in the system.

In the paper, the user group, and the BS group is defined as $\mathcal{N} = \{0, 1, ..., N-1\}$, $\mathcal{M} = \{0, 1, ..., M-1\}$. Furthermore, to express the muting bandwidth for m-th BS, $\bar{\mathcal{M}}_m$ is defined as $\bar{\mathcal{M}}_m = \{0, 1, ..., m-1, m+1, ..., M-1\}$.

III. Problem Description and Optimum Resource Allocation

A. Problem Description

The achievable data rates of the n-th user from the m-th BS via the non-muting bandwidth, $\mathcal{B}$ is defined as $r(m,n)$. Furthermore, the achievable data rates of the n-th user from the m-th BS via the muting bandwidth of the l-th BS, $\hat{\mathcal{B}}_l$, is defined as $\hat{r}(m,l,n)$.

The amount of bandwidth in $\mathcal{B}$, and $\hat{\mathcal{B}}_l$, assigned to the n-th user are defined as $b(m,n)$, and $\hat{b}(m,l,n)$, respectively. The throughput of the n-th user is calculated as

$$\zeta(n) = \sum_{m\in\mathcal{M}} b(m,n)r(m,n) + \sum_{m\in\mathcal{M}}\sum_{l\in\bar{\mathcal{M}}_m} \hat{b}(m,l,n)\hat{r}(m,l,n). \tag{1}$$

Based on the definition above, we can obtain the optimum resource allocation $b(m,n)$, and $\hat{b}(m,l,n)$, by calculating $b(m,n)$, and $\hat{b}(m,l,n)$, which maximize PF utility function

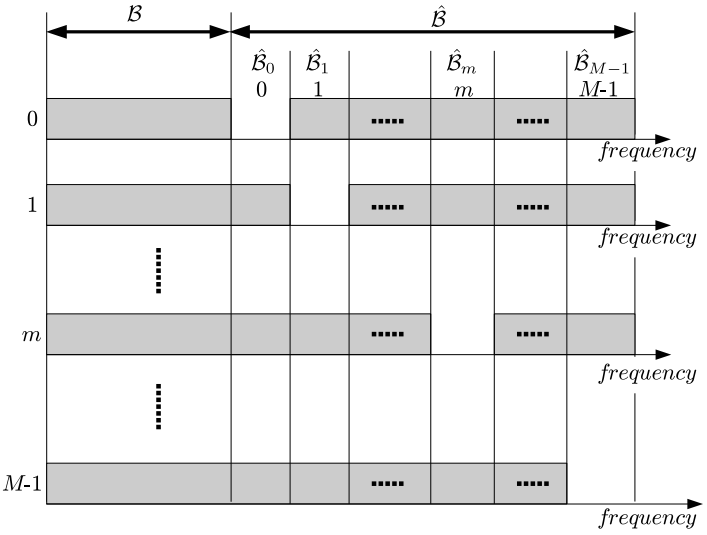

Fig. 2: System model.

[5]. It is described as the following *convex* optimization problem.

$$\text{maximize } F = \sum_{n\in\mathcal{N}} \log\zeta(n) \tag{2}$$

$$\text{subject to } b(m,n) \geq 0 \quad (m\in\mathcal{M}, n\in\mathcal{N}) \tag{3}$$

$$\hat{b}(m,l,n) \geq 0 \quad (m\in\mathcal{M}, l\in\bar{\mathcal{M}}_m, n\in\mathcal{N}) \tag{4}$$

$$\sum_{n\in\mathcal{N}} b(m,n) + \sum_{l'\in\bar{\mathcal{M}}_m}\sum_{n\in\mathcal{N}} \hat{b}(m,l',n) + \sum_{n\in\mathcal{N}} \hat{b}(l,m,n) = 1 \ (m\in\mathcal{M}, l\in\bar{\mathcal{M}}_m) \tag{5}$$

The first term of Eq.(5) represents the amount of the non-muting bandwidth. The second term denotes the summation of the muting bandwidth of l'-th BSs $(l'\in\bar{\mathcal{M}}_m)$. The third term represents the muting bandwidth of m-th BS.

B. Optimum Resource Allocation

In Eq.(2) to (5), the KKT conditions are the necessary and sufficient conditions for the optimum solution, since the PF utility function, F, is *convex*. The KKT conditions are described below.

$$\frac{r(m,n)}{\zeta(n)} = -\lambda_{(m,n)} + \mu_m \ (m\in\mathcal{M}, n\in\mathcal{N}) \tag{6}$$

$$\frac{\hat{r}(m,l,n)}{\zeta(n)} = -\hat{\lambda}_{(m,l,n)} + \mu_m + \mu_{(l,m)} \quad (m\in\mathcal{M}, l\in\bar{\mathcal{M}}_m, n\in\mathcal{N}), \tag{7}$$

$$\lambda_{(m,n)} b(m,n) = 0 \quad (m\in\mathcal{M}, n\in\mathcal{N}), \tag{8}$$

$$\lambda_{(m,n)} \geq 0 \quad (m\in\mathcal{M}, n\in\mathcal{N}), \tag{9}$$

$$\hat{\lambda}_{(m,l,n)}\hat{b}(m,l,n) = 0 \quad (m\in\mathcal{M}, l\in\bar{\mathcal{M}}_m, n\in\mathcal{N}), \tag{10}$$

$$\hat{\lambda}_{(m,l,n)} \geq 0 \quad (m\in\mathcal{M}, l\in\bar{\mathcal{M}}_m, n\in\mathcal{N}), \tag{11}$$

where $\mu_{(m,l)}$ is the Lagrange multiplier for equality constraint and $\lambda_{(m,n)}$, and $\hat{\lambda}_{(m,l,n)}$ are the multipliers for inequality

constraint. Furthermore, μ_m is defined as the summation of $\mu_{(m,l)}$, i.e.,

$$\mu_m = \sum_{l \in \bar{\mathcal{M}}_m} \mu_{(m,l)}. \tag{12}$$

By eliminating $\lambda_{(m,n)}$, and $\hat{\lambda}_{(m,l,n)}$, following equations are derived.

$$\begin{cases} b(m,n) = \max\left(0, \frac{1}{\mu_m} - \frac{\dot{\zeta}(m,n)}{r(m,n)}\right) \quad (m \in \mathcal{M}, n \in \mathcal{N}) \\ \hat{b}(m,l,n) = \max\left(0, \frac{1}{\mu_m + \mu_{(l,m)}} - \frac{\dot{\zeta}(m,l,n)}{\hat{r}(m,l,n)}\right) \\ \qquad\qquad (m \in \mathcal{M}, l \in \mathcal{L}_m, n \in \mathcal{N}) \end{cases}, \tag{13}$$

where $\dot{\zeta}(m,n)$, and $\dot{\zeta}(m,l,n)$ are defined as $\dot{\zeta}(m,n) = \zeta(n) - b(m,n)r(m,n)$, $\dot{\zeta}(m,l,n) = \zeta(n) - \hat{b}(m,l,n)\hat{r}(m,l,n)$, respectively.

The derived equations in Eq.(13) are similar to the well-known water-filling algorithm with the constraint of Eq.(5). From Eq.(13), to apply the water-filling algorithm for m-th BS, the resource allocation results, i.e., $\mu_{(m,l)}$ in other BSs are required. Therefore, when we calculate the $b(m,n)$ and $\hat{b}(m,l,n)$ for the m-th BS, we fix the $\mu_{(m',l)}$ in other BSs $(m' \neq m)$, and calculate them from Eq.(13). The process is performed for other BS, successively until the $b(m,n)$ and $\hat{b}(m,l,n)$ converges. This updating process is summarized in Algorithm 1.

In the updating process, $b(m,n)$, and $\hat{b}(m,l,n)$ need to be updated using Eq.(13). In other words, the unknown value, μ_m, need to be derived with the constraint of Eq.(5). In the paper, we will derive the updating process for $M = 2$, although it is possible to extend the general number of M. From Eq.(12), following equations are derived for $M = 2$,

$$\mu_0 = \mu_{(0,1)}, \quad \mu_1 = \mu_{(1,0)}. \tag{14}$$

Therefore, Eq.(13) is simplified as

$$\begin{cases} b(m,n) = \max\left(0, \frac{1}{\mu_m} - \frac{\dot{\zeta}(m,n)}{r(m,n)}\right) \\ \hat{b}(m,1-m,n) = \max\left(0, \frac{1}{\mu_0+\mu_1} - \frac{\dot{\zeta}(m,1-m,n)}{\hat{r}(m,1-m,n)}\right) \\ \qquad\qquad (m = 0,1, n \in \mathcal{N}) \end{cases}. \tag{15}$$

Eq.(15) is obtained by the water-filling algorithm with the multiple water levels as shown in Fig. 3. As shown in the figure, the hill level is defined as $\frac{\dot{\zeta}(m,n)}{r(m,n)}$, $\frac{\dot{\zeta}(m,1-m,n)}{\hat{r}(m,1-m,n)}$ for $n \in \mathcal{N}$. According to the decrease of μ_m, the water levels, i.e., $\frac{1}{\mu_m}$, $\frac{1}{\mu_0+\mu_1}$, increase, and the total number of users below water levels, K[1], increases. Finally, when the total amount of water satisfies Eq.(5), $b(m,n)$, $\hat{b}(m,1-m,n)$ is obtained, which satisfy Eq.(15) and (5).

Here, $\dot{\mu}(m,n)$ and $\dot{\mu}(m,1-m,n)$ are defined when the water level becomes equal level to the hill level, i.e., $b(m,n) = 0$, $\hat{b}(m,1-m,n) = 0$ in Eq.(13). $\dot{\mu}(m,n)$ and $\dot{\mu}(m,1-m,n)$ are described as

$$\dot{\mu}(m,n) = \frac{r(m,n)}{\dot{\zeta}(m,n)} \quad (n \in \mathcal{N}), \tag{16}$$

$$\dot{\mu}(m,1-m,n) = \frac{\hat{r}(m,1-m,n)}{\dot{\zeta}(m,1-m,n)} - \mu_{1-m} \quad (n \in \mathcal{N}). \tag{17}$$

[1]When both muting and non-muting resources are assigned to one user, such user is multiply counted in K.

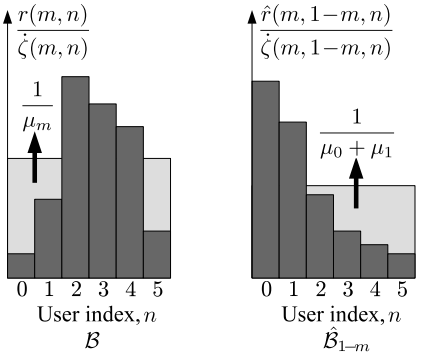

Fig. 3: Multiple water filling in Eq.(15) for m-th BS.

Furthermore, $\dot{\mu}(m,n)$ and $\dot{\mu}(m,1-m,n)$ are sorted in the descending order. Here, we define $\mathcal{R}$ as the user group which the users with positive $b(m,n)$ value in non-muting resource, $\mathcal{B}$, belong to. We also define $\hat{\mathcal{R}}_{1-m}$ as the user group which the users with positive $\hat{b}(m,1-m,n)$ value in muting resource, $\hat{\mathcal{B}}_{1-m}$, belong to. For example, $\mathcal{R} = \{0,1,5\}$, $\hat{\mathcal{R}}_{1-m} = \{2,3,4,5\}$ in Fig.3. By defining the number of users in $\mathcal{R}$ and $\hat{\mathcal{R}}_{1-m}$ as $|\mathcal{R}|$ and $|\hat{\mathcal{R}}_{1-m}|$, the total number of users below water levels, K is obtained as $K = |\mathcal{R}| + |\hat{\mathcal{R}}|$. Furthermore, the following equations are satisfied,

$$b(m,n) = \begin{cases} \frac{1}{\mu_m} - \frac{\dot{\zeta}(m,n)}{r(m,n)} & (n \in \mathcal{R}) \\ 0 & (n \notin \mathcal{R}) \end{cases}, \tag{18}$$

$$\hat{b}(m,1-m,n) = \begin{cases} \frac{1}{\mu_0+\mu_1} - \frac{\dot{\zeta}(m,1-m,n)}{\hat{r}(m,1-m,n)} & (n \in \hat{\mathcal{R}}_{1-m}) \\ 0 & (n \notin \hat{\mathcal{R}}_{1-m}) \end{cases}. \tag{19}$$

By substituting Eq.(18) and (19) into Eq.(5), Eq.(5) becomes

$$\frac{|\mathcal{R}|}{\mu_m} + \frac{|\mathcal{R}_{1-m}|}{\mu_0+\mu_1} - \sum_{n \in \mathcal{R}} \frac{\dot{\zeta}(m,n)}{r(m,n)} - \sum_{n \in \mathcal{R}_{1-m}} \frac{\dot{\zeta}(m,1-m,n)}{\hat{r}(m,1-m,n)} - 1 = 0. \tag{20}$$

Eq.(20) have a unique solution, since the left hand side of Eq.(20) monotonically decreases according to the increase of μ_m, if the appropriate K value is selected. Therefore, the solution is calculated by the numerical method such as Newton method, and can be verified by calculating $b(m,n)$ and $\hat{b}(m,1-m,n)$ in Eq.(15), and checking whether Eq.(5) is satisfied. This process is summarized in Algorithm 2.

Algorithm 1 Iterative algorithm

Initialize $b(m,n)$, $\hat{b}(m,l,n)$, $\zeta_0(n)$.
$i \leftarrow 0$.
repeat
  for $m = 0$ to $(M-1)$ **do**
    Update $b(m,n)$, $\hat{b}(m,l,n)$ from Algorithm 2.
  end for
  Update $\zeta_{i+1}(n)$ from Eq.(1).
  Calculate $\epsilon = \sum_{n \in \mathcal{N}} |\zeta_{i+1}(n) - \zeta_i(n)|$
  $i \leftarrow i + 1$.
until $\Delta \leq \epsilon$

Algorithm 2 Updating $b(m,n)$, $\hat{b}(m,1-m,n)$ using Eq.(15)

Initialize $b(m,n)=0$, $\hat{b}(m,1-m,n)=0$ for $n \in \mathcal{N}$.
$K \leftarrow 0$.
repeat
  $K \leftarrow (K+1)$.
  Calculate $\dot{\zeta}(m,n)$, $\dot{\zeta}(m,1-m,n)$.
  Calculate $\dot{\mu}(m,n)$, $\dot{\mu}(m,1-m,n)$ from Eq.(16), (17).
  Sort $\dot{\mu}(m,n)$, $\dot{\mu}(m,1-m,n)$ in descending order and define $\mathcal{R}$ and $\hat{\mathcal{R}}_{1-m}$.
  Calculate μ_m by Newton method assuming Eq.(20).
  Calculate $b(m,n)$, $\hat{b}(m,1-m,n)$ from Eq.(15).
  Calculate κ as the left hand side of Eq.(5).
until $\kappa = 1$

IV. Numerical Evaluation

In the paper, the simple environment using the one-dimensional model with two BSs ($M = 2$) is presented to show how the proposed scheme works. Table I shows the numerical evaluation parameters. In the evaluation, the achievable data rate is defined as $W \max(\log_2(1+\gamma), 8)$, where W and γ represent the number of subcarriers in total system bandwidth, and received signal-to-interference plus background noise power ratio, respectively[2].

Fig. 4 shows the achievable data rate normalized by the number of subcarriers in total system bandwidth as a function of location x. In the figure, $r_m(x)$, and $\hat{r}_m(x)$ denote the achievable data rate per subcarrier connecting to m-th BS without DPS/DPB, and that with DPS/DPB, respectively. Furthermore, the BS-1 and BS-2 are located at $x = 0$ and 500(m). As shown in the figure, according to the increase of the distance from the BS, the achievable data rate decreases. However, by employing the DPS/DPB, the achievable data rate is kept high value.

TABLE I: Numerical Evaluation Parameters

Parameter	Value
Number of subcarrier per system bandwidth	600
Inter-cell distance	500 m
Transmission power of BS	46 dBm
Antenna pattern	Omni antenna
Antenna gain of BS	14 dBm
Pathloss model	37.6log R +128.1 dB
Antenna gain of user	0 dBi
Thermal noise density	-174 dBm/Hz
Number of users	10

Next, we will show the allocation results in the following two cases.

- **Case 1:** Users are equally distributed between BS-1 and BS-2.
- **Case 2:** More users are located close to BS-1.

Fig.5 shows the resource allocation results obtained by the proposed scheme for Case 1. The upper part of the graph represents the ratio of muting and non-muting resources for both BS. The lower part of the graph represents the resource allocation for respective users. The x axis represents the user location, and the bar height in y axis represents the amount of allocations. Different colors shows the different BS and with/without DPS/DPB. In the figure, all bars contain the single color, which represents that only one of the BSs is allocated to each user, and only one transmission method is applied, although Eq.(1) does not restrict such allocations. Furthermore, the amount of resource allocation is even for all users without DPS/DPB, although the achievable data rate is not equal. As expected, the DPS/DPB is employed for the users located at the cell boundary, since the data rate improvement by employing the DPS/DPB is high (See Fig. 4). The resource allocation is completely same for BS-1 and 2, due to the assumption of the equal user distributions.

[2]We assume maximum modulation level as 256QAM and coding rate of one.

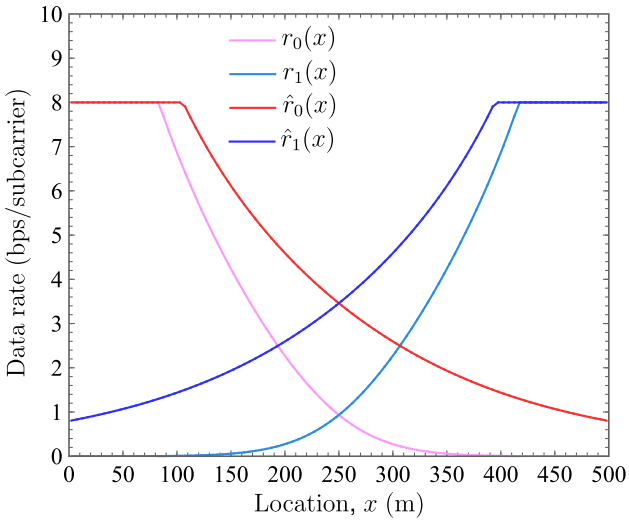

Fig. 4: Data rate as a function of location x.

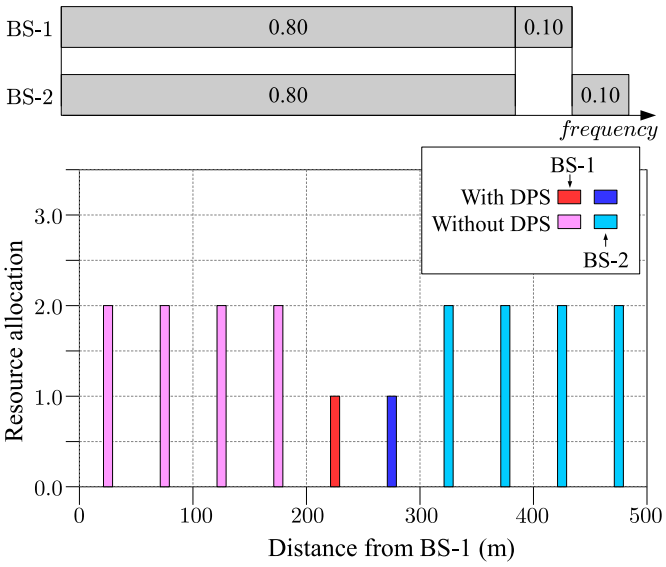

Fig. 5: Resource allocation results (Case 1).

Fig.6 shows the resource allocation results obtained by the proposed scheme for Case 2, where more users are located close to BS-1. As shown in the upper part of the graph, the BS-2 performs DPB, although BS-1 does not. This is because it is beneficial to improve PF metric by performing DPB in BS-2 only to compensate for the unequal user distributions.

From these results, it is confirmed that the proposed scheme works well. However, in the actual system, the proposed scheme can not be applied, since it only works for the *average* data rate, not instantaneous data rate. However, there are two possible applications. One application is the CoMP user candidates selection. The DPS/DPB user candidates need to measure the instantaneous data rate with and without DPS/DPB of all BS candidates, and feed back these informations to the BSs in the uplink channel. When too large number of users are selected as the DPS/DPB user candidates, the feedback uplink channel reduces the uplink data channel, the complex scheduling is required. On the other hand, when too small number of users are selected, the DPS/DPB gain cannot be obtained. Therefore, the extension of the proposed scheme will be beneficial. Another application is the ICIC, which is generally controlled in the slow time scale, such as more than 100 msec. Therefore, this scheme can be applicable for the ICIC.

From the discussion above, the proposed scheme is effective to perform DPS/DPB and its extension for other applications is presented.

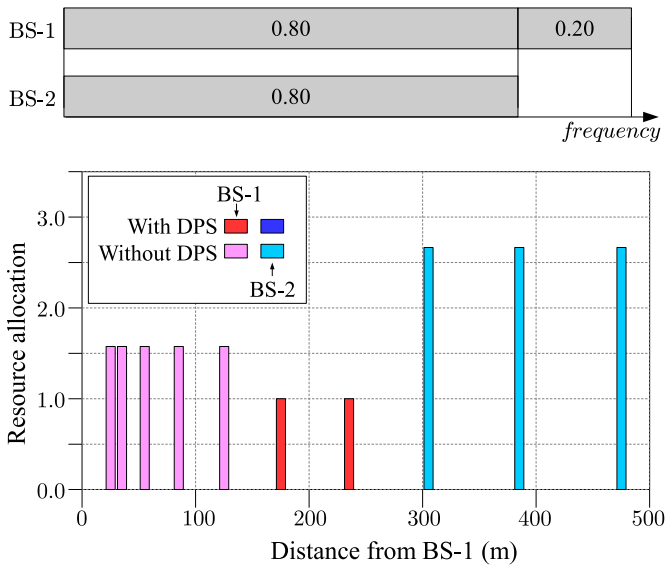

Fig. 6: Resource allocation results (Case 2).

V. Conclusion

This paper investigated the DPS/DPB, since it can achieve superior performance with relatively small overhead among CoMP transmission schemes, which is one the of promising techniques to increase the throughput of users located at the cell-edge. This paper proposed the DPS/DPB scheme based on the PF criteria. We derived the optimum DPS/DPB allocation scheme by extending the work in [7], and solving the *convex* optimization problem based on the achievable *average* data rate of each user. The simple environment using the one-dimensional model with two BSs was presented, and showed that the proposed scheme works well. Furthermore, the extension of the proposed scheme to select the DPS/DPB user candidates, and to the ICIC, was presented.

References

[1] NTT DOCOMO, "DOCOMO 5G white paper," 2014. [Online]. Available: https://www.nttdocomo.co.jp/english/corporate/technology/whitepaper_5g/

[2] A. Alexiou, "Wireless World 2020: Radio Interface Challenges and Technology Enablers," *IEEE Veh. Technol. Mag.*, vol. 9, no. 1, pp. 46–53, Mar. 2014.

[3] D. Lee, H. Seo, B. Clerckx, E. Hardouin, D. Mazzarese, S. Nagata, and K. Sayana, "Coordinated multipoint transmission and reception in LTE-advanced: Deployment scenarios and operational challenges," *IEEE Commun. Mag.*, vol. 50, pp. 148–155, 2012.

[4] H.-L. Määttänen, K. Hämäläinen, J. Venäläinen, K. Schober, M. Enescu, and M. Valkama, "System-level performance of LTE-Advanced with joint transmission and dynamic point selection schemes," *EURASIP J. Adv. Signal Process.*, vol. 2012, no. 1, p. 247, Nov. 2012.

[5] F. Kelly, "Charging and rate control for elastic traffic," *Eur. Trans. Telecommun.*, vol. 8, no. 1, pp. 33–37, Jan. 1997.

[6] L. Liu and J. Zhang, "Proportional fair scheduling for multi-cell multi-user MIMO systems," in *2010 44th Annu. Conf. Inf. Sci. Syst.* IEEE, Mar. 2010, pp. 1–6.

[7] H. Seki, T. Kobayashi, and D. Kimura, "Selection of Component Carriers Using Centralized Baseband Pooling for LTE-Advanced Heterogeneous Networks," *IEICE Trans. Commun.*, vol. E96-B, no. 6, pp. 1288–1296, 2013.

[8] M. R. Jeong and N. Miki, "A Simple Scheduling Restriction Scheme for Interference Coordinated Networks," in *2012 IEEE Veh. Technol. Conf. (VTC Fall)*. IEEE, Sep. 2012, pp. 1–6.

[9] T. Oyama and H. Seki, "Small Cell Design with Cooperative Transmission for LTE-Advanced Heterogeneous Networks," in *IEICE Tech. Rep. SR2014-80*, 2014.

[10] M. Sternad, T. Ottosson, A. Ahlen, and A. Svensson, "Attaining both coverage and high spectral efficiency with adaptive OFDM downlinks," in *2003 IEEE 58th Veh. Technol. Conf. VTC 2003-Fall*, vol. 4. IEEE, 2003, pp. 2486–2490 Vol.4.

Acknowledgement

This work was partially supported by grants from the Sanyo Broadcasting Foundation.